UNIVERSIDAD NACIONAL DE COLOMBIA
SEDE MEDELLÍN
FACULTAD DE MINAS

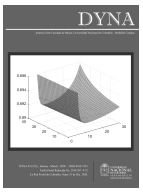

DYNA
http://dyna.medellin.unal.edu.co/

MPM and ALE simulations of large deformations geotechnics instability problems

Giovanna Monique Alelvan [a], Daniela Toro-Rojas [a], Amanda Cristina Pedron Rossato [b], Raydel Lorenzo Reinaldo [b] & Manoel Porfirio Cordão-Neto [a]

[a] *Postgraduate program in Geotechnic, University of Brasilia, Brasilia, Brazil. giovannaalelvan@gmail.com, dtr1593@gmail.com, porfirio@unb.br*
[b] *Civil Engineering program, Federal University of Tocantins, Tocantins, Brazil. amandacristinarossato@gmail.com, raydellr@gmail.com*

Received: July 9th, 2019. Received in revised form: February 6th, 2020. Accepted: February 18th, 2020

Abstract
Problems involving large deformations are the focus of numerical modeling researches in recent decades due to the challenge of finding a kinematic appropriate description of the continuum. In recent years, different formulations have been used to describe such problems as the Arbitrary Lagrangian Eulerian (ALE) method and the Material Point Method (MPM). These two methods allow to perform dynamic analyzes involving large deformations. In this way, this work aims to present a comparison of problems applied to Geotechnics involving large deformations and large displacements, using MPM and FEM associated with the ALE method. For this purpose, three problems have been simulated: sliding of blocks on an inclined plane, runout process of sand and instability of a slope using the MPM and the FEM associated with the ALE method. In all cases, a comparison of the results is presented, and the advantages and disadvantages of each method are discussed.

Keywords: large deformations; material point method; finite element method; arbitrary Lagrangian Eulerian.

Simulaciones de problemas de grandes deformaciones en geotecnia usando MPM y ALE

Resumen
Los problemas que involucran grandes deformaciones son el foco de las investigaciones de modelos numéricos en las últimas décadas debido al desafío de encontrar una descripción cinemática adecuada del continuo. En los últimos años, se han utilizado diferentes formulaciones para describir problemas como el método Euleriano Lagrangiano Arbitrario (ALE) y el Método del Punto Material (MPM). Estos dos métodos permiten realizar análisis dinámicos que involucran grandes deformaciones. De esta forma, este trabajo pretende presentar una comparación de problemas aplicados a la geotecnia que involucran grandes deformaciones y grandes desplazamientos, utilizando MPM y el Método de los Elemento Finitos (FEM) asociado con el método ALE. Para este propósito, se simulan tres problemas: deslizamiento de bloques en un plano inclinado, deslizamiento de arena e inestabilidad de una pendiente utilizando el MPM y el FEM asociado con el método ALE. En todos los casos se presenta una comparación de los resultados y se discuten las ventajas y desventajas de cada método.

Palabras clave: grandes deformaciones; método del punto material; método de los elementos finitos; Lagrangiano Euleriano arbitrario.

1. Introduction

Problems involving large deformations are the focus of numerical modeling researchers in recent decades due to the challenge of finding a kinematic appropriate description of the continuum. This description determines the relationship between the deformation of the body and the finite element mesh or the background mesh [1].

Algorithms used in continuum mechanics problems, in general, use two classic descriptions of movement: the

How to cite: Alelvan, G.M, Toro-Rojas, D, Rossato, A.C.P, Lorenzo, R. and Cordão-Neto, M, MPM and ALE simulations of large deformations geotechnics instability problems. DYNA, 87(212), pp. 226-235, January - March, 2020.

Lagrangian and the Eulerian. In the first, all the nodes of the mesh are associated with a particle of the material during the analysis. The second use a fixed background mesh and the continuous moves on it [1].

The Finite Element Method (FEM) has its formulation based on the continuum mechanics and traditionally uses the Lagrangian description [2]. However, in analyzes involving large deformations, the distortion of the finite element mesh results in a lack of reliable results [3]. On the other hand, the Eulerian description has the disadvantage of not allowing the variables evaluation in the same point of the material with the passage of time [4].

In the last years new formulations have been presented to describe problems of large deformations. Among them, those that combine the advantages of classical descriptions such as the Coupled Eulerian-Lagrangian (CEL) and Arbitrary Lagrangian Eulerian (ALE) methods have emerged. In addition to these, mesh-free methods like the Smooth Particle Hydrodynamics (SPH) and the Particle Finite Element Method (PFEM); and mesh and particle methods, such as the Material Point Method (MPM).

Slope instability problems are examples of geotechnical problems that involve large displacement and have negative socio-economic impact. In the last years, the analysis of this type of problems has been approached using several methodologies and numerical modeling has been shown as one of the most effective tools to study the possible impacts caused by landslides. [5-7].

In this way, this work aims to present a comparison of problems applied to Geotechnics involving large deformations and large displacements, using MPM and FEM associated with the ALE method. The objective is to evaluate advantages and disadvantages of each of the methods in large deformations problems. For this, the software ANURA3D® and ABAQUS® [8,9] were used. The cases studied address difficulties that are presented in numerical modeling of landslides problems and offer an analysis of the situations encountered.

1.1. Finite element method and arbitrary Lagrangian Eulerian method

As the configuration of the body changes during the analysis, it is necessary to establish the configuration that will be used as a reference to describe the continuum mechanics equations. [10] presented two well-known methods that allowed large deformations and large displacements, which are: Total Lagrangian (TL) and Updated Lagrangian (UL). The methods differ according to the reference configuration used, with the initial TL and the UL being updated in the time frame.

According to [2], TL and UL are two different ways of linearizing the equilibrium equation and must lead to the same solution of the problem. In theory, these approaches should be able to solve problems of large deformations. However, according to the author, they lose accuracy and convergence when large distortions occur in the mesh.

In order to overcome this inefficiency of TL and UL methods, the Arbitrary Lagrangian-Eulerian Method (ALE) was developed. This method can be seen as a combination between the Lagrangian and Eulerian descriptions, by using the advantages of both to solve the problem of finite element mesh distortion [2].

Unlike the TL and UL methods, the ALE does not use a fixed reference system in space or to the body. The system used by ALE is called the Computational Reference System (CRS). In this, the position of the points is not given and can be fixed in space or in the body, depending on the stage of analysis.

This re-meshing process is arbitrary, as the name of the method itself suggests; there are several possibilities to find an optimized mesh for the problem. Although arbitrary, the new mesh must meet two criteria: adapt to the contour of the domain, and the typology and the connectivity of the mesh must remain the same as the previous one. These requirements must be guaranteed to allow the mapping of the variables from the old to the new mesh [2].

In ABAQUS® software two fundamental steps must be evaluated in ALE properties: creation of the new mesh and transfer of state variables from old to new through a process called advection. The creation of a new mesh is not done in all the steps of an analysis, and then to define the time interval with which this happens it is necessary to inform the update frequency value of the mesh [8].

In this way, during a step of time with ALE, that is, where the creation of a new mesh will be made, two processes are executed: scanning of the old mesh and advection of the variables for the new mesh. The mesh scanning process is done iteratively on the ALE domain. During each mesh scan, the domain nodes are relocated, based on their position and adjacent ones to reduce distortion in the element. After the process of relocation of the mesh nodes, the mapping of the state variables of the old mesh to the new one is done by the process called advection sweep [8].

1.2. Material point method

The MPM appears as an alternative to the FEM, which can use many of the concepts used in the FEM but without the mesh distortion problems [11]. MPM blends ideas and procedures from the Particle-in-cell Method (PIC) and the FEM. With this method, the bodies are discretized as a group of unconnected particles, which carry a mass whose value is kept fixed to guarantee the conservation of the mass. The other parameters necessary to define the state of the body, such as stress, density and variables history are also associated with material points [12].

The interaction between the particles in the MPM is made at the nodes of a stationary Eulerian computational grid, which remains constant for the entire calculation, thus eliminating distortion problems (Fig. 1). The mesh is then used to determine the incremental solution of the governing equations by Eulerian description [13].

In MPM the motion equations are solved in this computational mesh that covers the entire domain of the problem. At each step of the analysis, the interpolation

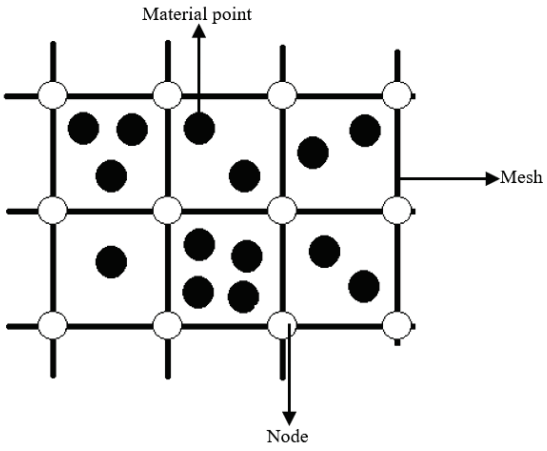

Figure 1. Discretization using the Material Point Method
Source: The Authors.

between the variables carried by the material points and the mesh nodes is done, using the associated functions, similar to the FEM.

The boundary conditions are imposed on the mesh nodes and the motion equations are solved incrementally. Therefore, the magnitudes of the variables in the material points are updated, by weighing the results of the nodes, again using the same form functions. In MPM the information stored in the mesh is not required in the next step of the analysis, so it can be discarded [14].

The MPM has been used to simulate different geotechnical problems such as landslides [15], foundations [16], anchor modeling in soils [17], modeling of excavator loads [18], granular flow problems in a silo [19], simulation of tests related to deformations induced by failures movements [20], analysis of propagation of soil flows induced by earthquakes [21], geomembrane response to settlements [22] and slip problems with coupled flow [23].

2. Numerical models

To evaluate the capacity of FEM and MPM to treat problems involving large deformations, three numerical models were used: block sliding on an inclined plane, sand sliding and slope instability. The first model presents analytical solution. The second model reproduces a small-scale test presented by [7]. The last model is studied only comparatively among the numerical methods used. The models using FEM were made in ABAQUS / Explicit® software and MPM in ANURA3D® software.

2.1. Case 1: sliding blocks on an inclined plane

This case is a reproduction of an example of the ANURA3D® software manual. The objective of this model is to validate the ability of the methods to perform dynamic analyzes with mass movements and with different friction coefficients between the blocks and the sliding surface.

The model consists of an inclined plane, with three blocks

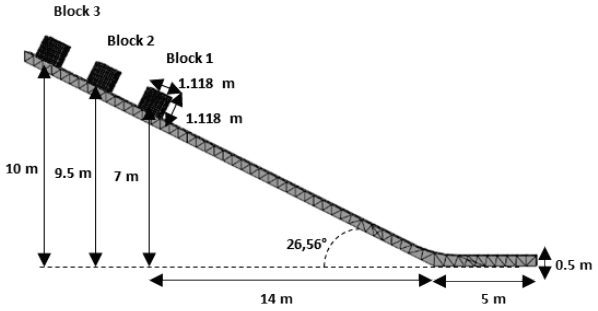

Figure 2. Initial configuration of the sliding blocks
Source: The Authors.

sliding over it. The blocks have a density of 2000 kg/m³, a Poisson coefficient of 0.33 and a Young Module of 20000 kPa. The plane has a density of 4000 kg/m³, a Poisson coefficient of 0.33 and a Young Module of 40000 kPa. The model geometry is shown in Fig. 2.

The inclined plane has two regions with different friction coefficients: the upper one, which has a friction angle of 0.3, 0.325 and 0.35 with blocks 1, 2 and 3, respectively; and the lower one, which presents a friction coefficient of 0.45 with all the blocks.

The model was made in finite element software following the properties described above. As a boundary condition, the plane was restricted in all directions, and the blocks were only perpendicular to the direction of movement. An interface was inserted between the blocks and the two regions of the planes, with the friction values as shown. The gravitational field was applied during the analysis.

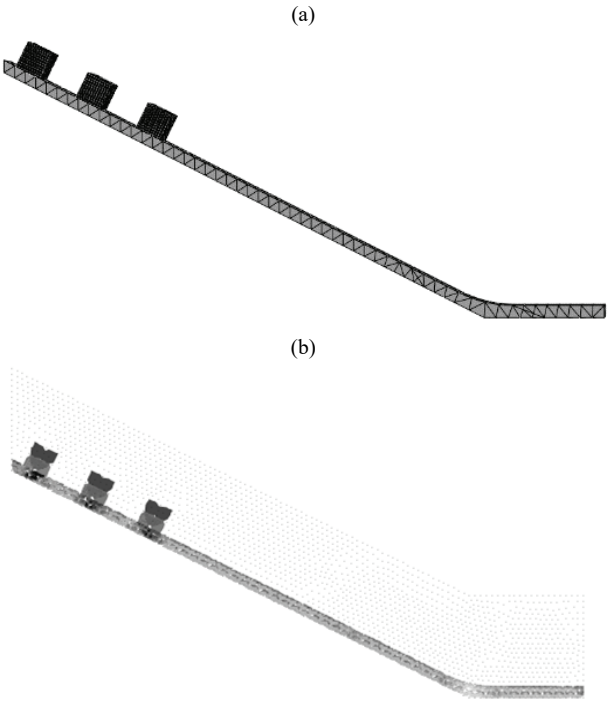

Figure 3. Initial configuration of the sliding blocks: (a) finite element method (b) material point method.
Source: The Authors.

The C3D10M (10-node modified quadratic tetrahedron) elements of the software library were used in the blocks and in the plane. In the blocks the mesh size was 0.11 m, resulting in 5399 nodes and 3418 elements. The mesh of the plane has size of 0.5 m, which generated 1155 nodes and 422 elements. The finite element mesh can be visualized in Fig. 3a. This mesh was defined after a mesh density analysis process.

In the model using MPM, ten material points per cell were used in the blocks and four material points in the inclined plane. The bottom mesh was generated with 2910 tetrahedral and semi-structured elements totaling 6207 nodes. The initial configuration of the blocks is shown in Fig. 3b.

The simulation was done in two phases: in the first one the initial stresses were generated by a quasi-static gravitational load and in the second the contact formulation was inserted allowing the sliding of the blocks by the inclined plane. In each phase a quantity of time steps was established: 1 and 70, for step 1 and step 2, respectively. Throughout the analysis a local damping factor of 0.05 was considered to avoid oscillation problems.

2.1.1. Results

The displacement results of the blocks on the inclined plane are shown in Figs. 4 and 5 presents the velocity results.

(a)

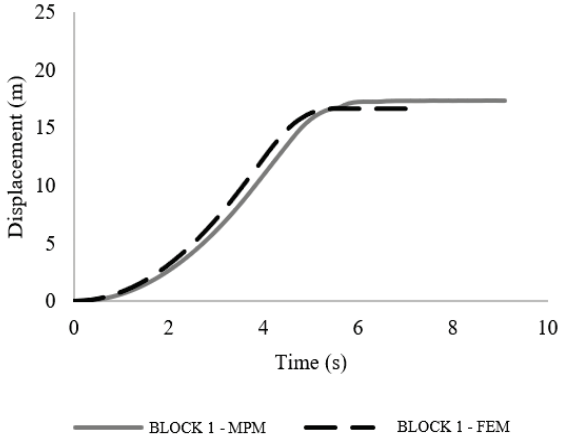

(b)

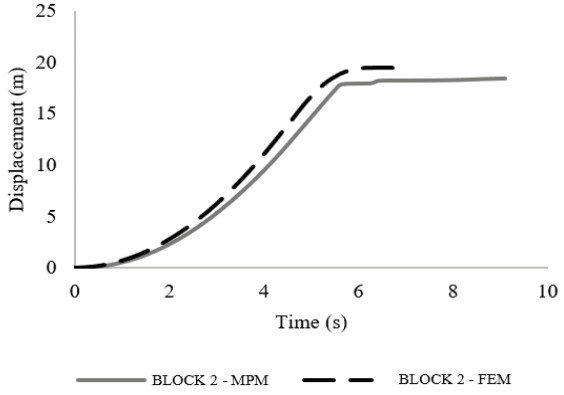

(c)

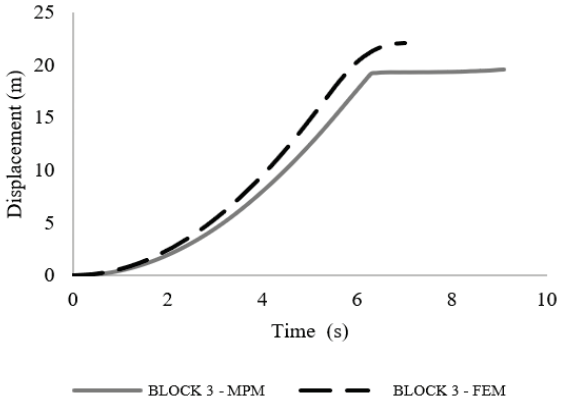

Figure 4. Horizontal velocity of the blocks. (a) block 1; (b) block 2; (c) block 3.
Source: The Authors.

(a)

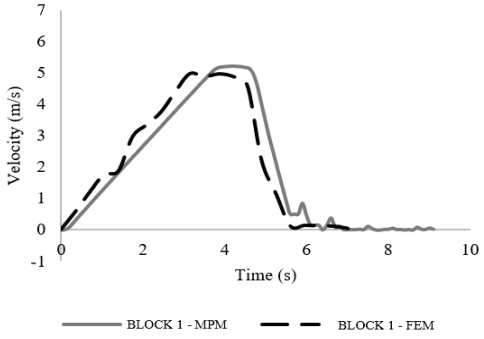

(b)

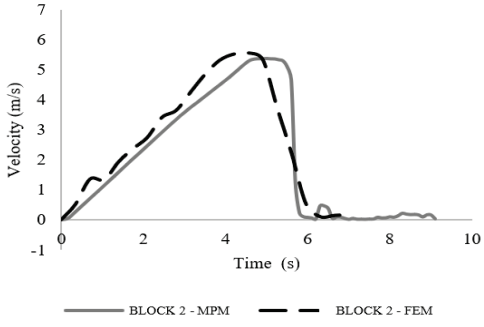

(c)

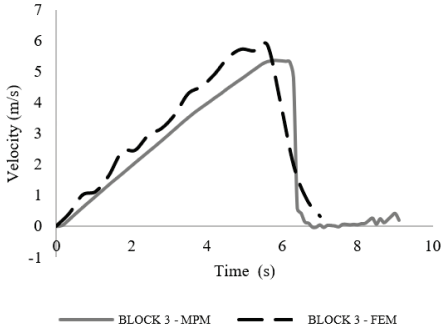

Figure 5. Horizontal displacement of the blocks. (a) block 1; (b) block 2; (c) block 3.
Source: The Authors.

From the analysis of the presented graphs and due to the agreement of the results, it is contacted that the methods are able to carry out analyzes with mass movements. It is observed that the horizontal displacements obtained by the methods were approximated for all the blocks, as well as for the acceleration and velocity. In the velocity and acceleration graphic for block 1 there is an oscillation in the results using MPM. This can be caused due to numerical instability generated by the collision between block 1 and the others.

2.2. Case 2: runout process of sand

[7] analyzed the behavior of wet and dry sand sliding through small-scale experimental tests. For this, an experimental box with a stainless-steel inclined flow channel and acrylic side walls was used. At the end of the channel, a simple base was placed to carry out the measurements of reach and configuration of the sliding mass. The geometry of the model is shown in Fig. 6.

The dry sand tested by [7] had a grain diameter of D50 of 0.34 mm. The sand was compacted at a relative density of 60% before being released into the stream. The volume used was 6000 cm³. The internal friction angle of the sand was 35.91 °. The distances reached by the flow were captured by the video cameras at the top of the box and with this the distance vs. time graph was obtained.

In this work, numerical models were performed from the [7] experimental data for dry sand with a 30º box inclination. Elastic behavior for the channel and elastoplastic for the sand with Mohr-Coulomb failure criterion was allowed. The soil and channel properties are shown in Table 1.

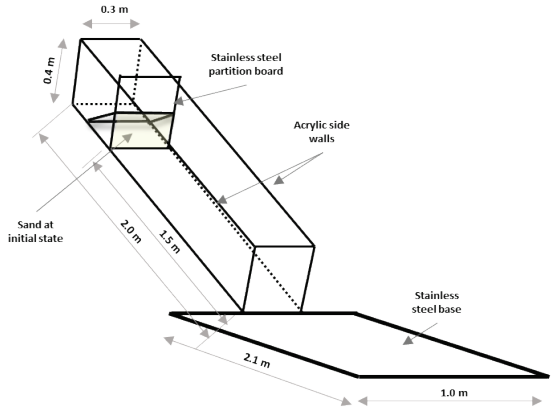

Figure 6. Initial configuration of the sliding sand.
Source: The Authors.

Table 1.
Mass and channel properties

Properties	Sand	Channel
Density	1543 kg/m³	2500 kg/m³
Poisson	0,3	0,3
Young Modulus (E)	5 MPa	10^7 MPa
Friction angle	35,9°	-
Cohesion	0 kPa	-

Source: Adapted from [7].

In this model using the FEM was necessary to associate the properties of the ALE, since the large deformations in the sand mass lead to distortions in the finite element mesh, which may cause numerical instability. In this way, the update of the mesh made it possible to simulate the slip test described.

The analysis was performed in two phases: in the first, both the mass and the channel had restricted the displacements in all directions; in the second, the displacement of the sand in the downward direction of the channel was allowed, allowing the sliding.

For the finite element mesh, C3D8R elements with a size of 0.04 m for the channel and 0.01 m for the sand were used, which resulted in 11966 nodes and 400 elements in the soil; 918 nodes and 400 elements in the inclined channel; and 2756 nodes and 1300 elements in the horizontal base of the channel.

Regarding the properties of the ALE, to improve represent the test, the frequency of the mesh update was every five calculation steps. For the mesh smoothing methods, only the volume smoothing method was used and for the advection process, the second order method was chosen.

In the model using MPM, 29536 tetrahedral elements were used. In addition, for the sand, 10 particles were used per element and 4 particles per element were inserted into the channel. The damping used was 0.05.

Fig. 7 shows the mass configurations for the experimental model and numerical models. The FEM / ALE model was able to predict the sliding of the mass only up to 1.2 s, and in the MPM the simulation was able to go to the final phase of the test (2.1 s).

The FEM / ALE model was able to simulate only up to t = 1.2 s due to finite element mesh distortion, resulting from large mass deformations. It was noticed that these distortions occurred mainly in the change of surface slope, which made the ALE not able to maintain the quality of the finite element mesh.

In MPM, numerical instability was also observed during the passage of material points from the inclined surface to the

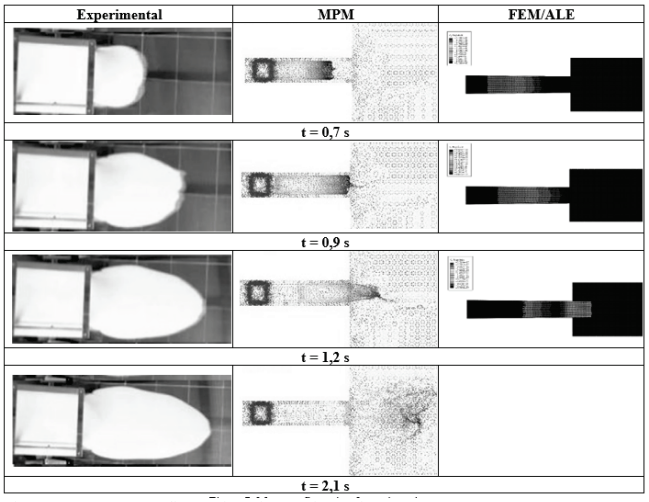

Figure 7. Mass configuration for various times.
Source: The Authors.

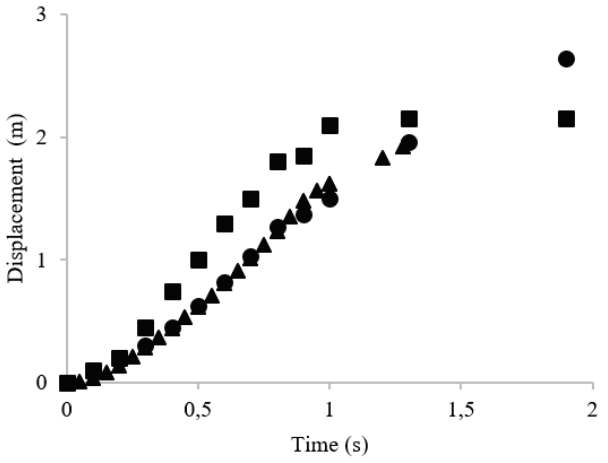

Figure 8. Comparison of the distance reached by the sand mass.
Source: The Authors.

horizontal. This fact may have happened through the transition of the material points from one mesh to another, since the mesh used in the channel has different dimensions from the horizontal box. No reference to the numerical problem was found in the literature. Lastly, the sand displacement results obtained in the experimental box and the ALE and MPM models are shown in Fig. 8.

Although MPM and FEM / ALE failed to adequately reproduce the sand spreading pattern (Fig. 7), the displacements obtained numerically were very close to each other.

2.3. Case 3: slope failure

In order to evaluate the mass movement due to a slope failure, models were made whose instability was generated by the action of gravity. The model studied is a slope of 4 m high and 45 ° slope. The soil mass lies on a foundation of 1 m in height and 10 m in length. The boundary effect was considered as having no influence on the results.

Regarding the materials, the foundation was admitted with linear elastic behavior and elastoplastic for slope with Mohr-Coulomb rupture criterion. The other properties for the slope are: density 2200 kg/m³, Poisson 0,33, Young Module 32800 kPa, Friction angle 31° and cohesion 0. For the foundation: density 2800 kg/m³, Poisson 0,33, Young Module 4000000 kPa.

As a boundary condition, the total displacements of the foundation and the horizontal displacements of the side of the slope were restricted. For MPM the analysis was closed when the ruptured soil ceased the movement, that is, it had velocity zero. As for the FEM model, the analysis was conducted until it was completed by the software due to excess deformation in the finite element mesh.

As in the previous model, to perform this type of analysis using the FEM it is necessary to associate the ALE method properties. Thus, using the geometry and properties of the presented materials, it was established that the re-meshing would occur in all increments. The other ALE properties were the same as the previous model. In the finite element mesh 4096 triangular elements were used CPE3 (3-node linear plane strain triangle), with a size of 0.1 m, which generated 2181 nodes.

Even with a frequency equal to one, that is, performing the re-meshing in all increments, the analysis was interrupted by the software at t = 1.3s due to excessive distortion in the finite element mesh, and the model did not represent the real behavior. Fig. 9 presents this analysis with the occurrence of mesh distortion especially at the base of the slope, for three different periods of time of the analysis.

Due to this limitation of the method, it was decided to create the rupture surface and allow the mass to move. This surface was defined by the concentration of plastic shear deformations presented in the continuous analysis, according to Fig. 10.

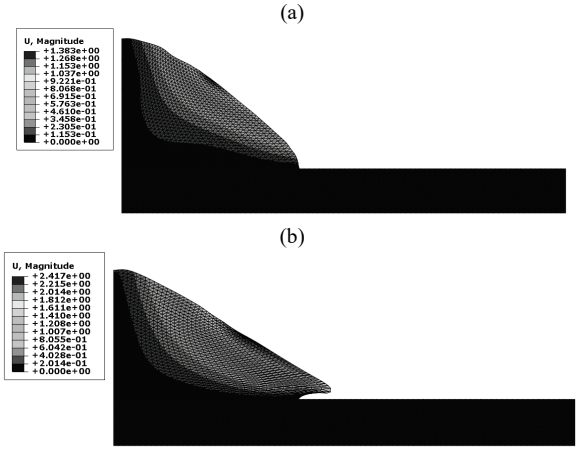

Figure 9. Displacement (m) and finite element mesh distortion. (a) 0,75 s; (b) 1,3 s.
Source: The Authors.

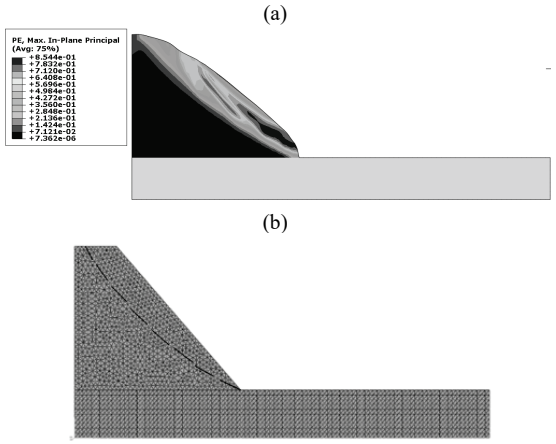

Figure 10. Rupture surface. (a) concentration of plastic shear strains; (b) predefined surface.
Source: The Authors.

Once the surface was defined, a new interface was created between the sliding and the intact mass. The interface friction angle was considered equal to the internal friction angle of the soil (31º). The analysis was conducted in two phases: first established the equilibrium, and then allowed the mass downward movement.

The density and topology of the finite element mesh were maintained. However, an interface has been inserted between the sliding mass and the foundation, to avoid a numerical error of meshes overlapping between the parts. For the ALE parameters, a frequency of five was adopted.

In the model using the MPM were inserted in the slope and foundation four material points per cell. In addition, a background mesh with 60450 elements and 90783 nodes was generated to allow movement and update of the points position and all variables at each instant of time.

The simulation was done in two phases: the first one generates the state of initial stress in two steps of time of 1.0s each; in the second stage, gravity failure was simulated, and 50 steps of analysis with a time per step of 0.05 seconds were used to visualize the displacement of the mass in greater detail.

In this case, the influence of damping on slip development was also evaluated. With high values (0.7-0.9), the problem is considered and simulated as quasi-static, impeding correct analysis of the total dynamic behavior of mass movement.

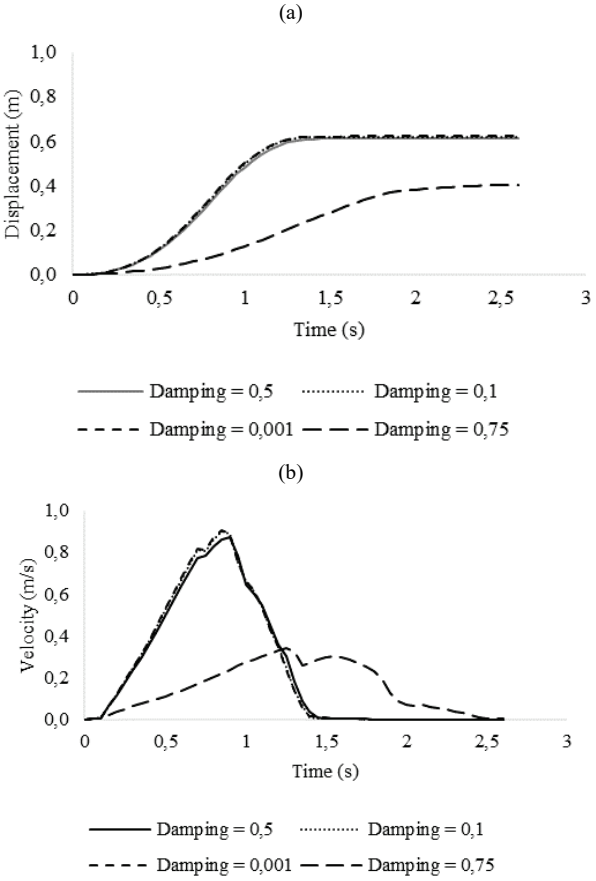

Figure 11. Evaluation of damping influence. (a) displacement; (b) velocity.
Source: The Authors.

On the other hand, with lower values (0.05-0.15), it is possible to simulate the energy dissipation of the material, which also allows a better evaluation of the movement. This was observed in the results presented in Fig. 11, where the displacements and velocities of the evaluated points were higher with low damping due to the more accurate representation of the phenomenon, and smaller with high damping due to the proximity to a static situation that accelerates the convergence, reducing the movement range.

2.3.1. Results

For the slope model, the evolution of the displacement for the model in MPM is presented in Fig. 12. The total distance covered by the mass on the foundation is 2.40 m, corresponding to a length shorter than the total height of the slope.

Fig. 13 shows the evolution of the displacement at different times for the model in FEM / ALE. The total distance covered on the foundation was 2.30 m, which is also lower than the total height of the slope, and close to that obtained by MPM.

Observing the rupture surface formed by the MPM (Fig. 14a) it is noted that has a configuration similar to the one obtained by FEM, through the concentration of shear strains. In addition, comparing the evolution of both methods, the MPM and the FEM predicted the formation of a dead zone, that is, particles with zero velocity.

The range of the ruptured mass was approximated for both methods. Thus, to a better evaluation of the soil regions, three monitoring points were selected: top, middle and basement of the slope. The displacement and velocity for these points are shown in Figs. 14 and 15, respectively.

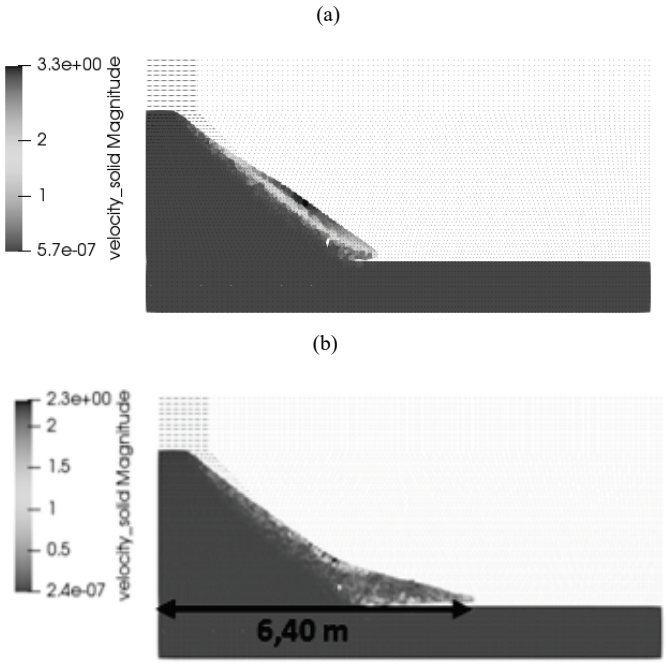

Figure 12. Mass displacement. (a) t=1,40 s; (b) 2,60 s;
Source: The Authors.

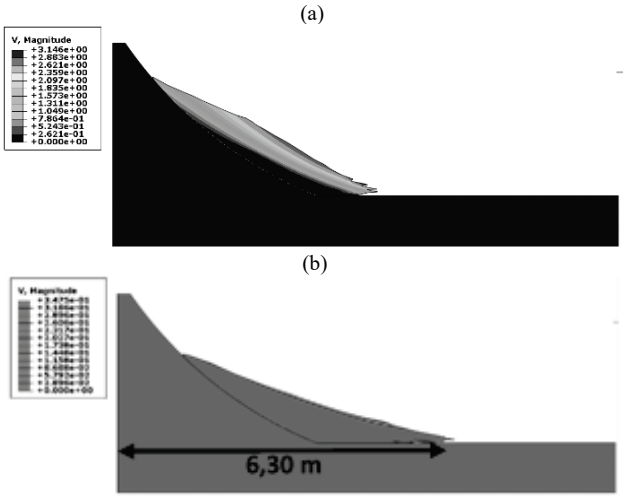

Figure 13. Velocity of the mass. (a) t=1,40 s; (b) 3 s;
Source: The Authors.

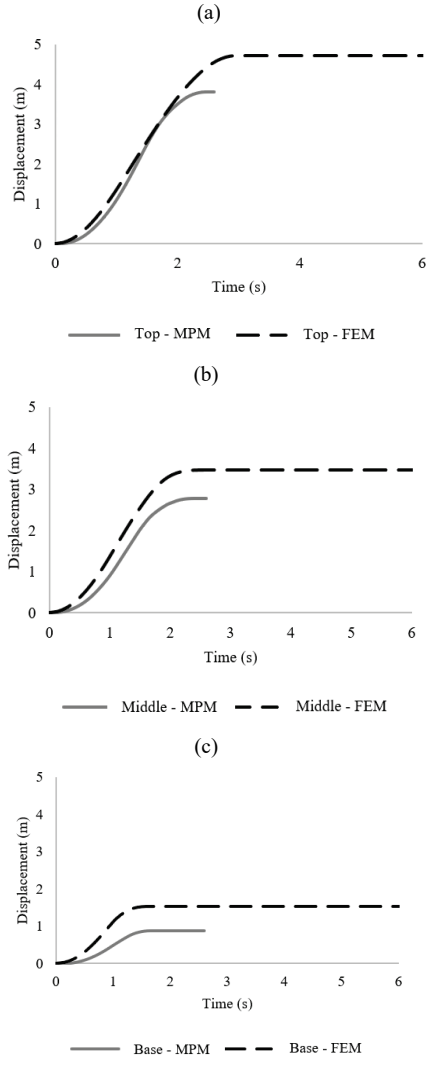

Figure 14. Displacement of the top, middle and bottom points of the sliding mass. (a) Top; (b) Middle; (c) Base.
Source: The Authors.

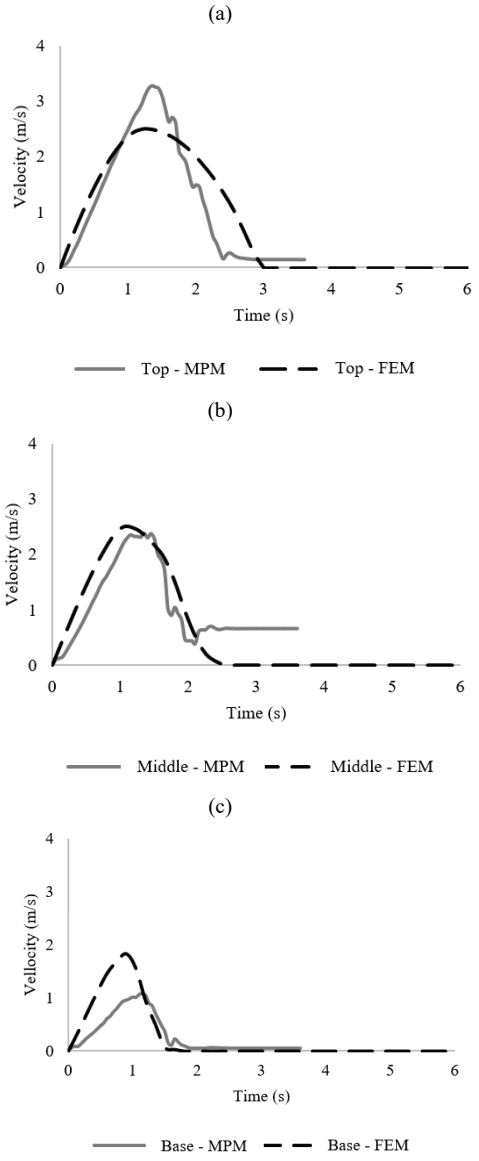

Figure 15. Velocity of the points on the top, middle and the base of the sliding mass. (a) Top; (b) Middle; (c) Base.
Source: The Authors.

From the results of displacement and velocity it is observed that the points of the top of the slope are those that have greater displacement and speed. On the other hand, the lower soil portion of the slope moves less and with less velocity, and therefore, forms the dead zone.

The results of the points were similar for the methods, but the FEM / ALE analysis led to approximately 0.7 meters over maximum displacement in the three regions analyzed. Regarding velocity, the middle points in both methods had approximate results, however, for the base the FEM / ALE predicted higher velocities and to the top the MPM.

This behavior is explained by the fact that the movement in the FEM / ALE is similar to a single deformable body, in this way, the points of the base move on the foundation until

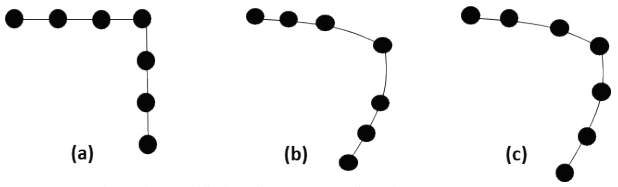

Figure 16. Relocation of finite element mesh using ALE (a) contours before deforming; (b) after deformation; (c) after relocation
Source: The Authors.

they lose velocity. This is a characteristic of the method to consider the continuum, and also due to the re-meshing process, which happens from the positioning of the adjacent nodes. This means that from the movement of one node, the other will follow so that the mesh topology is maintained, as shown in Fig. 16.

In the case of MPM, because it is a semi-continuous method, the particles are free to move in any region of the calculation mesh. In this way, in a few increments they contribute to the formation of the dead zone, that is, a region with zero velocity points.

3. Conclusions

Problems involving large deformations are common in Geotechnics and should be increasingly explored. Especially for slope rupture verification, which poses a risk of material damage and loss of human life. In this work it was possible to evaluate the capacity of the FEM and MPM in analyzes involving large deformations. In the first model of blocks on an inclined plane it was observed that both methods represented the problem well, but the FEM has a lower computational cost than the MPM, so it is a better alternative.

In the second model of sand sliding on a channel, it was observed that MPM was closer to the experimental solution. Despite this, both methods had problems in the change of channel slope: in the MPM related to alteration in the size of the background mesh; and in the FEM / ALE the updating of the mesh due to the large deformations.

Finally, in the slope model, it was found that MPM represents the phenomenon better because it is not necessary to preset the rupture surface. In addition, the analysis by this method was able to predict the full reach of the mass, while in the FEM / ALE it was aborted by excess deformation.

The damping value placed on the dynamic problems has a great influence on the result, in general low values must be added in order not to create an excessive damping of the problem and consequently to erroneous results.

Acknowledgments

The authors would like to thank the Graduate Program in Geotechnical Engineering, Coordination for the Improvement of Higher Education Personnel (CAPES) and National Council for Scientific and Technological Development (CNPq) for the financial support of the research.

References

[1] Donea, J., Huearta, A., Ponthot, J. and Rodríguez-Ferran, A., Arbitrary Lagrangian-Eulerian methods, Chapter 14, Encyclopedia of Computational Mechanics, Edited by Erwin Stein, René de Borst and Thomas J.R. Hughes. Volume 1: Fundamentals, 2004, ISBN: 0-470-84699-2.

[2] Nazem, M., Sheng, D. and Carter, J.P., Stress integration and mesh refinement for large deformation in geomechanics, International Journal for Numerical Methods in Engineering, 65, pp. 1002-1027, 2006. DOI: 10.1002/nme.1470

[3] Nazem, M. and Sheng, D., Arbitrary Lagrangian-Eulerian method for consolidation problems in geomechanics, in: VII International Conference on Computational Plasticity, COMPLAS VII, CIMNE, Barcelona, 2005.

[4] Sheng, D., Nazem, M. and Carter, J.P., Some computational aspects for solving deep penetration problems in geomechanics, Computational Mechanics, 44, pp. 549-561, 2009. DOI: 10.1007/s00466-009-0391-6

[5] Ceccato, F. and Simonini, P., Numerical based design of protection systems against landslides. Conference on Numerical Methods in Geotechnics. TUHH, Hamburg, Germany, 2017.

[6] Gabrieli, F. and Ceccato, F., Impact of dry granular flows on a rigid wall: discrete and continuum approach. In: VI Italian Conference of Researchers in Geotechnical Engineering, Padova, Italia, 2016.

[7] Abe, K and Konagai, K., Numerical simulation for runout process of debris flow using depth-averaged material point method. Soils and Foundations, 56(5), pp. 869-888, 2016. DOI: 10.1016/j.sandf.2016.08.011

[8] ABAQUS. Abaqus Analysis User's Guide, [online]. 2014. [Access: July of 2018] Available at: http://130.149.89.49:2080/v6.14/books/usb/default.htm?startat=pt05ch22s07abm13.html

[9] Anura3D. Anura3D MPM Software - Tutorial Manual. Anura3D MPM Research Community, 2017.

[10] Bathe, K.J., Ramm, E. and Wilson, E.L., Finite element formulations for large deformations dynamic analysis, International Journal for Numerical Methods in Engineering, 9, pp. 353-386, 1975. DOI: 10.1002/nme.1620090207

[11] Sulsky, D., Chen, Z. and Schreyer, H.L., A particle method for history-dependent materials. Computer Methods in Applied Mechanics and Engineering, 118, pp. 176-196, 1994.

[12] Zabala, F. and Alonso, E.E., Progressive failure of Aznalcóllar dam using the material point method. Geotechnique 61(9), pp. 795-808, 2011. DOI: 10.1680/geot.9.P.134

[13] Al-Kafaji, I., Formulation of a dynamic material point method (MPM) for geomechanical problems. Dr. Thesis. Stuttgart University, Germany, 2013.

[14] Zabala, F., Modeling hydro-mechanical geotechnical problems using the material point method. Dr. Thesis. Universidad Politécnica de Cataluña, Cataluña, Spain, 2010.

[15] Llano, M., Muniz, M. and Martinez, H., Numerical modelling of Alto Verde landslide using the material point method. DYNA 82(193), pp. 150-159, 2015. DOI: 10.15446/dyna.v82n194.48179

[16] Lorenzo, R., Pinto, R., Cordão, M. and Nairn, J.A., Numerical simulations of deep penetration problems using the material point method. Geomechanics and Engineering 11(1), pp. 59-76, 2016. DOI: 10.12989/gae.2016.11.1.059

[17] Coetzee, C.J., Vermeer, P.A. and Basson, A.H., The modelling of anchors using the material point method. International Journal for Numerical and Analytical Methods in Geomechanics, 29(9), pp 879-895, 2005. DOI: 10.1002/nag.439

[18] Coetzee, C.J., Basson, A.H. and Vermeer, P.A., Discrete and continuum modelling of excavator bucket filling. Journal of Terramechanics, 44(2), pp 177-186, 2006. DOI: 10.1016/j.jterra.2006.07.001

[19] Wieckowski, Z., Modelling of silo discharge and filling problems by the material point method. TASK Quarterly, [online]. 7(4), pp. 701-21, 2003. Available at: http://task.gda.pl/quart/index.html

[20] Johansson, J. and Konagai, K., Fault induced permanent ground deformations: experimental verification of wet and dry soil, numerical findings relation to field observations of tunnel damage and implications for design. Soil Dynamics and Earthquake Engineering.

27(10), pp. 938-956, 2007. DOI: 10.1016/j.soildyn.2007.01.007
[21] Konagai, K., Johansson, J. and Itoh, H., Pseudo-three-dimensional Lagrangian particle finite difference method for modeling earthquake induced soil flows, in: 13th World Conference on Earthquake Engineering. No 547, 2004.
[22] Zhou, S., Stormont, J. and Chen, Z., Simulation of geomembrane response to settlement in landfills by using the material point method. International Journal for Numerical and Analytical Methods in Geomechanics, 23(15), pp. 1977-1994, 1999.
[23] Soga, K., Alonso, E., Yerro, A., Kumar, K. and Bandara, S., Trends in large-deformation analysis of landslide mass movements with particular emphasis on the material point method. Geotechnique, 11, pp. 1-26, 2015. DOI: 10.1680/jgeot.15.LM.005
[24] Nazem, M., Daichao, S., Carter, J.P. and Sloan, S.W., Arbitrary Lagrangian-Eulerian method for large-strain consolidation problems. International Journal for Numerical and Analytical Methods in Geomechanics. 32, pp. 1023-1050, 2008. DOI: 10.1002/nag.657

G.M. Alelvan, she holds a MSc. at Geotechnical Engineering by the University of Brasilia, Brazil, and BSc. Eng. in Civil Engineering by the Federal University of Uberlandia, Brazil. Currently she is developing research in numerical modelling, focusing on mass movements and natural disasters.
ORCID: 0000-0003-0665-0664

D. Toro-Rojas, she holds a MSc. at Geotechnical Engineering by the University of Brasilia, Brazil, and BSc. Eng. in Civil Engineering by the Pilot University of Colombia, Colombia. Currently she is developing research in numerical modelling, mass movements, natural disasters and pavements.
ORCID: 0000-0002-4896-0532

A.C.P. Rossato, she holds a BSc. Eng. in Civil Engineering by Federal University of Tocantins (UFT), Brasil.
ORCID: 0000-0002-0910-2156

R. Lorenzo, he holds a Dr. in Geotechnics by University of Brasília, Brazil, a MSc. in Soil Mechanics and Geotechnical Engineering in 2010, from the Polytechnic University of Madrid, Spain, and BSc. Eng. in Civil Engineering in 2006, from the Instituto Superior Politecnico Jose Antonio Echeverria, Cuba.
ORCID: 0000-0003-2419-9758

M, Cordão-Neto, he holds a Dr. in Geotechnics, and a MSc. in Geotechnics, all of them from the University of Brasília, Brazil. Is a BSc. Eng. in Civil Engineering and BSc. in Data Processing, all of them form the State University of Piaui, Brazil. He has postdoctoral in 2008, from the University of Strathclyde, UK.
ORCID: 0000-0003-0618-4376